



Analysis of Endocannabinoid System in Rat Testis During the First Spermatogenetic Wave

Marina Migliaccio¹, Giulia Ricci², Antonio Suglia¹, Francesco Manfredola¹, Ken Mackie³, Silvia Fasano¹, Riccardo Pierantoni¹, Teresa Chioccarelli^{1†} and Gilda Cobellis^{1*†}

¹ Department of Experimental Medicine, Sez. Bottazzi, Università degli Studi della Campania "L. Vanvitelli", Naples, Italy,

² Department of Experimental Medicine, Laboratorio di Istologia ed Embriologia, Università degli Studi della Campania

"L. Vanvitelli", Naples, Italy, ³ Department of Psychological and Brain Sciences, Indiana University, Bloomington, IN, United States

OPEN ACCESS

Edited by:

Vance Trudeau,
University of Ottawa, Canada

Reviewed by:

Giovanna Berruti,
Università degli Studi di Milano, Italy
Sigrid Hoyer-Fender,
Georg-August-Universität
Göttingen, Germany

*Correspondence:

Gilda Cobellis
gilda.cobellis@unicampania.it

[†]These authors have contributed
equally to this work.

Specialty section:

This article was submitted to
Experimental Endocrinology,
a section of the journal
Frontiers in Endocrinology

Received: 11 January 2018

Accepted: 08 May 2018

Published: 29 May 2018

Citation:

Migliaccio M, Ricci G, Suglia A,
Manfredola F, Mackie K, Fasano S,
Pierantoni R, Chioccarelli T and
Cobellis G (2018) Analysis of
Endocannabinoid System in Rat
Testis During the First
Spermatogenetic Wave.
Front. Endocrinol. 9:269.
doi: 10.3389/fendo.2018.00269

Endocannabinoids are lipid mediators, enzymatically synthesized and hydrolyzed, that bind cannabinoid receptors. Together with their receptors and metabolic enzymes, they form the "endocannabinoid system" (ECS). Anandamide (AEA) and 2-arachidonoylglycerol (2-AG) are the main endocannabinoids studied in testis. In this study, using the first wave of spermatogenesis as an *in vivo* model to verify the progressive appearance of germ cells in seminiferous tubules [i.e., spermatogonia, spermatocytes, and spermatids], we analyzed the expression of the main enzymes and receptors of ECS in rat testis. In particular, the expression profile of the main enzymes metabolizing AEA and 2-AG as well as the expression of cannabinoid receptors, such as CB1 and CB2, and specific markers of mitotic, meiotic, and post-meiotic germ cell appearance or activities have been analyzed by RT-PCR and appropriately correlated. Our aim was to envisage a relationship between expression of ECS components and temporal profile of germ cell appearance or activity as well as among ECS components. Results show that expression of ECS components is related to germ cell progression. In particular, CB2 and 2-AG appear to be related to mitotic/meiotic stages, while CB1 and AEA appear to be related to spermatogonia stem cells activity and spermatids appearance, respectively. Our data also suggest that a functional interaction among ECS components occurs in the testis. Indeed, *in vitro*-incubated testis show that AEA-CB2 activity affects negatively monoacylglycerol-lipase levels *via* upregulation of CB1 suggesting a CB1/CB2-mediated relationship between AEA and 2-AG. Finally, we provide the first evidence that CB1 is present in fetal gonocytes, during mitotic arrest.

Keywords: testis, endocannabinoid system, spermatogenesis, germ cells, CB1, CB2

INTRODUCTION

Spermatogenesis is a complex biological process including proliferation, meiosis, and differentiation of germ cells, from spermatogonia (SPG) stem cells to spermatozoa (SPZ). The proliferation phase starts during the embryonic development (1). In rat, proliferating primordial germ cells reach the genital ridges at 10.5 days post coitum (*dpc*). They colonize the differentiating gonad and, triggered by the testicular microenvironment (2–4), start proliferating to give rise to gonocytes. Proliferation ends at 18.5 dpc, when gonocytes enter G1/G0 mitotic arrest (5). At 3 days post partum (*dpp*), gonocytes resume the cell cycle and, after DNA synthesis, are blocked in G2 phase. On 4–5 *dpp*, germ

cells migrate toward the basement of seminiferous tubules and enter mitosis establishing the initial pool of unipotent SPG stem cells (5). This self-renewal activity produces undifferentiated SPG (i.e., proSPG) which differentiate (commitment in type A1 SPG) and proliferate (A1-A4-B SPG) before starting meiosis as spermatocytes (SPC) (around 10–12 *dpp*). Spermatids (SPT) are produced (around 26 *dpp*), then they differentiate in SPZ (around 45 *dpp*) through a dramatic reorganization involving both the nuclear and cytoplasmic compartments (6, 7).

Spermatogenesis is finely regulated by various hormones and factors that act through endocrine, autocrine, and paracrine pathways (8, 9–20). Among these, endogenous cannabinoids (i.e., endocannabinoids) are lipid mediators emerging as modulators of spermatogenesis (21–25) and reproduction (26–28). The endocannabinoids are produced “on demand” from membrane phospholipids. They bind and activate type-1 (CB1) and type-2 (CB2) cannabinoid receptors (29, 30) mimicking some effects of Δ^9 -tetrahydrocannabinol, the psychoactive component of the *Cannabis sativa*. Arachidonylethanolamine (i.e., anandamide, AEA), and 2-arachidonoylglycerol (2-AG) are the main endocannabinoids identified in vertebrates (31, 32); their synthesis is mainly catalyzed by NAPE-hydrolyzing phospholipase D (NAPE-PLD) (33) and *sn*-1-DAG-lipase (DAGL) (34), respectively. Their degradation is controlled by two specific enzymes: the fatty acid amide hydrolase (FAAH) that preferentially degrades AEA (2-AG at less extent) while the monoacylglycerol-lipase (MAGL) hydrolyzes 2-AG (35, 36). The biosynthetic/hydrolyzing enzyme balance regulates the endocannabinoid content determining the appropriate “tone,” which is critical for many physiological processes (37, 38), including reproduction (39, 40). Receptors, endocannabinoid membrane transporter, ligands, and their metabolic enzymes form the “endocannabinoid system” (ECS) (41).

Many studies have been carried out to analyze expression and function of ECS in the male reproductive tract (42–51). The components of this system have been identified in mammalian and non-mammalian testes, in somatic and germ cells, from SPG to SPZ (21, 43, 44, 46, 49–56). CB1 has been localized in differentiating/mature adult Leydig cells, in SPT and SPZ and it seems to be positively related to (i) steroidogenesis (20–22, 56) and differentiation (49) of Leydig cell, (ii) chromatin remodeling (7, 57) of SPT, and (iii) maturation and quality of SPZ (44, 46, 47, 51, 52, 54, 55, 58). Interestingly, in rat testis, a weak and stage-specific expression of CB1 has been observed in Sertoli cells (22, 49) when SPT appear in seminiferous tubules. Study about CB1 activity in these cells is lacking. CB2 is highly expressed in murine SPG and SPC (a weak signal appears in SPT), and also in Sertoli cells isolated from 7, 16, and 18 *dpp* old mouse (43, 50). Data obtained from mice show that CB2, autocrinally activated by 2-AG, has a role in SPG proliferation and meiotic entry (50, 59). Indeed, 2-AG levels are high in SPG and dramatically decrease in SPC and round SPT (50). On the contrary, AEA levels mainly remain unchanged in germ cells, from SPG-to-SPT. However, Leydig and Sertoli cells contain AEA (21, 43). In Sertoli cells, a complete biochemical machinery to transport/degrade and to bind AEA *via* CB2 is present (43). AEA shows pro-apoptotic effects on Sertoli cells. Lower levels of AEA correlate with Sertoli

cell age and higher levels of FAAH suggesting a protective and pro-survival role of FAAH in these cells (48).

In this study, using the first wave of spermatogenesis as an *in vivo* model to study the progressive appearance of germ cells in seminiferous tubules (i.e., SPG, SPC, and SPT), we analyzed the expression of the main enzymes and receptors of ECS in rat testis. Our aim was to study the expression ECS components in testis during progressive appearance germ cells and to find a relationship between expression of ECS components and germ cell activity (i.e., mitosis, meiosis, SPT–SPZ differentiation).

MATERIALS AND METHODS

Experimental Animals

Experiments were approved by the Italian Ministry of Education and the Italian Ministry of Health. All methods and all animal procedures were performed in accordance with the relevant guidelines and regulations by National Research Council's for Care and Use of Laboratory Animals (NIH Guide).

Sprague-Dawley rats (*Rattus norvegicus*, from Charles River Laboratories, Lecco, Italy) and mice (*Mus musculus*) genetically deleted of CB1 in heterozygous conditions (CB1^{+/-}), provided by Prof. Ledent [knock out has been obtained by replacing the first 233 codons of CB1 gene with PGK-Neo cassette (60)], were kept in a room with controlled temperature (22 ± 2°C), ventilation, and lighting (12-h light/dark cycles) and were maintained on a standard pellet diet with free access to water. Male and female heterozygous CB1 mice will be bred on a CD1 background (Charles River Laboratories, Lecco, Italy) to expand colony, then used to generate WT and CB1^{+/-} male mice available for *in vitro* experiments.

Pregnant rats were sacrificed at 19.5 *dpc* and fetal testes from male embryos (*n* = 4) were collected and fixed for immunohistochemistry. Male rats were killed at 1, 7, 14, 21, 27, 31, 35, 41, 60 and 90 *dpp* and testes rapidly removed, frozen on dry ice, and properly stored for RT-PCR analyses. At least three animals/age were analyzed and at least one testis/animal separately processed for RT-PCR analysis.

Adult (6–8 months) male mice CB1^{+/-} were killed by CO₂ asphyxia, and testes processed for *in vitro* tissue incubation. Each experimental analysis included at least three testis/experimental group from different animals, and each testis/animal was separately analyzed.

Total RNA Preparation

Total RNA was isolated from rat testes using TRIZOL[®] Reagent (Invitrogen Life Technologies, Paisley, UK) according to the manufacturer's recommendations. To remove potential contamination of genomic DNA, RNA aliquots (10 µg) were treated with 2 U DNase (RNase-free DNase I, Ambion, Thermo Fisher Scientific, MA, USA) according to the manufacturer's recommendations. Purity and integrity of RNA samples were determined as previously reported (61).

RT-PCR Analysis

Semi-quantitative RT-PCR is a specific technique although less sensitive as compared with Real Time PCR. This allows one

to appreciate gene expression differences, just when these are evident and stable. Using RNA from whole testis, we consider this method to robustly run correlation tests of gene expression. To reinforce our methodological choice, we currently compared our data with those reported by Grimaldi characterizing ECS components in isolated mouse germ cells (50).

As already reported (49), total RNA (2 µg) was used to synthesize cDNA in 20 µl mix containing: 0.5 µg oligo dT, 10 mM dNTP, 0.01 M DTT, 1× first strand buffer (Invitrogen Life Technologies, Paisley, UK), 40 U RNase Out (Invitrogen Life Technologies, Paisley, UK), 200 U SuperScript-III RNaseH-Reverse Transcriptase (Invitrogen Life Technologies, Paisley, UK). As a negative control, total RNA (2 µg) was incubated in the previous mix without adding Reverse Transcriptase enzyme (RT – cDNA sample). PCR was carried out using 2 µl cDNA and 10 pmol of the appropriate primers in a PCR mix [0.2 mM dNTP, 1× PCR buffer (Invitrogen Life Technologies, Paisley, UK)], using an Applied Biosystem Thermocycler. Possible residual genomic DNA was evaluated using *Actin* primers by RT– cDNA amplification (at 35 cycles) while possible contamination among samples was excluded using samples prepared with 1 µl water (H₂O samples, negative control) in place of cDNA. Except for CB1 gene, primers were specifically designed on different exons (i.e., amplicons would span an intron if genomic DNA was amplified). Their sequences and PCR program are reported in **Table 1**. Each cDNA was amplified in duplicate or triplicate, in three independent experiments, and analyzed by electrophoresis on an agarose gel. Signals were quantified by densitometry analysis and graphed as optical density (OD) values normalized relatively to *Actin* (normalized OD values) amplified at 25 cycles by excluding the saturation phase.

The genotype of CB1^{+/-} testes was verified by PCR analysis of genomic DNA using specific primers for neomycin-cassette and CB1 gene (**Table 1**).

Immunocytochemistry (ICC)

Testes from 14.5 and 19.5 *dpc* rat embryos and 90 *dpp* rat were fixed overnight in Bouin's solution and embedded in paraffin using standard procedures, as previously described (38, 62). Microtome sections (5-µm thick) were stained with hematoxylin & eosin or incubated overnight with primary antibody solution [rabbit anti-human N-terminus CB1; diluted 1:500 (63)], rabbit anti-human NAPE-PLD (diluted 1:100 #10305, Cayman, MI, USA), rabbit anti-rat FAAH (diluted 1:500; #101600, Cayman, MI, USA), rabbit anti-rat MAGL (diluted 1:100, #24701, Abcam, Cambridge, UK) in 0.01 M PBS, 1% Triton-X100, 10% BSA (49). Immunoreactivity was revealed using the avidin–biotin complex system and H₂O₂/DAB (3,3'-diaminobenzidine-tetrahydrochloride) as substrate/chromogen. The specificity of immunoreaction has already been demonstrated (27, 28, 49, 51) and here routinely checked by omitting primary antibody. Sections were observed under a light microscope (Leica CTR500) and images captured using a high resolution digital camera (Leica DC300F).

Correlation Curves

Data of gene expression (normalized OD values, from three to five independent RT-PCR analyses) concerning ECS components

TABLE 1 | Primer sequences (S: sense; AS: antisense), annealing temperature (T_m) and cycles number used to analyse testicular levels of *Nape-pld*, *Faah*, *Magl*, *Dagl*, *Cb1*, *Cb2*, *Cxcl12*, *Mlh3*, *Hsp70t*, and *Actin* mRNA by RT-PCR.

Gene primers	Sequences 5'–3'	T _m (°C)	No. cycles	Product size (bp)
<i>Neomycin</i> S	gatccagaacatcaggtagg	56	35	521
<i>Neomycin</i> AS	aaggaaggggtgagaacagag			
* <i>Cb1</i> S	catcatcacagattctatgtac	56	35	366
* <i>Cb1</i> AS	gaggtgccaggagggaacc			
<i>Nape-pld</i> S	agatggctgataatggagaa	56	35	463
<i>Nape-pld</i> AS	ttctctcccaccagtc			
<i>Faah</i> S	ggaagtgaacaaagggacca	60	35	220
<i>Faah</i> AS	actgacattggcggcagcat			
<i>Dagl</i> S	cacgaggcctgctcctgaa	60	35	218
<i>Dagl</i> AS	gtgagccagacgatgccac			
<i>Magl</i> S	ggtcaatgcagacggacagt	64	35	303
<i>Magl</i> AS	atggagtggcccaggaggaa			
<i>Cb1</i> S	atctagatggccttgacaga	56	35	300
<i>Cb1</i> AS	taaagttctcccacactgga			
<i>Cb2</i> S	ggcagcgtgaccatgacct	60	35	406
<i>Cb2</i> AS	gacgtgaggtggccaagac			
<i>Cxcl12</i> S	ccagtcagcctgagctac	58	35	235
<i>Cxcl12</i> AS	gtctactggaaagtcctttg			
<i>Mlh3</i> S	gactaagagtattgtggagg	58	35	213
<i>Mlh3</i> AS	gcacactgaaatggcagct			
<i>Hsp70t</i> S	ggtgatgagggtctgaag	52	35	421
<i>Hsp70t</i> AS	gggtgggggtgtgaaaac			
<i>Actin</i> S	ctcttcagccttcctctct	60	25	298
<i>Actin</i> AS	ctgctgtgatccacatc			

In table are also indicate primer sequences for neomycin-cassette and CB1 gene (*) used for genotyping CB1^{+/-} mice. Product size indicate base pairs of the amplified fragments.

(*Nape-pld*, *Faah*, *Dagl*, *Magl*, *Cb1*, *Cb2* mRNA, as well as *Dagl*/*Magl* ratio mRNA, here used as index of intra-testicular 2-AG levels) and germ cell activity markers [chemokine (C-X-C motif) ligand 12 (*Cxcl12*); mutL homolog 3 (*Mlh3*); and a mouse testis-specific heat shock 70 protein (*Hsp70t*) mRNA] were conveniently compared, within specific time frames of the first spermatogenic wave, using the Excel built-in distribution functions available in Microsoft Office. The “*r*” value was considered to establish the test significance. The range $-1 \leq r \leq 1$ established negative or positive correlation.

In Vitro Testes Incubations and Western Blot Analysis

Anandamide and AM630 (6[6-iodo-2-methyl-1-[2-(4-morpholinyl)ethyl]-1H-indol-3-yl](4-methoxyphenyl)-methanone), a selective CB2 inverse agonist, were obtained from Sigma-Aldrich (Milan, Italy). Both drugs were of the purest analytical grade and each were dissolved in ethanol (i.e., AEA) or dimethylsulfoxide (DMSO; i.e., AM630) according to the manufacturer's instructions.

CB1^{+/-} testes with a feeble notch in tunica albuginea ($n = 3$ or 4 for experimental group) were incubated in PBS (6 ml) for 90 min with vehicle (0.015% ethanol plus 0.05% DMSO according to relative compound concentrations; control group) or with AEA (1 µM) ± AM630 (10 µM). Ethanol (0.0015%) and DMSO

(0.05%) were added in each experimental group. AM630 was always added 30 min before AEA at a concentration useful to affect CB2 activity as previously reported in cell cultures and *in vitro* testis (57, 64, 65) as well as in *in vivo* mice (59). Each testis/experimental group was separately homogenized in RIPA buffer [PBS, pH 7.4, 10 mM dithiothreitol, 0.02% sodium azide, 0.1% SDS, 1% Nonidet P-40, 0.5% sodium deoxycholate, in the presence of protease inhibitors (10 µg/ml of leupeptin, aprotinin, pepstatin A, chymostatin, and 5 µg/ml of TPCK)], as already reported (54) and analyzed by Western blot. Briefly: proteins (90 µg) were separated by SDS-PAGE (10% acrylamide) and transferred to polyvinylidene difluoride membrane (GE Healthcare) at 280 mA for 2.5 h at 4°C. Membrane was cut at 50-kDa level. The upper and lower filters were treated for 3 h with blocking solution [5% nonfat milk, 0.25% Tween-20 in Tris-buffered saline (TBS, pH 7.6)] and then separately incubated overnight, at 4°C in TBS-milk buffer (TBS pH 7.6, 3% nonfat milk) with different primary antibody [MAGL, diluted 1:500, code ab24701 from Abcam, Cambridge, UK; ERK1/2, diluted 1:1,000, code sc-154 from Santa Cruz Biotechnology, Inc., Heidelberg, Germany; CB1 C-terminal (46), diluted 1:1,000]. After washing in 0.25% Tween20-TBS, filters were incubated with 1:1,000 horseradish peroxidase-conjugated rabbit IgG (Dako Corp., Milan, Italy) in TBS-milk buffer and then washed again. The immune complexes were detected using the enhanced chemiluminescence-Western blotting detection system (Amersham ECL Western Blotting Detection Reagent, cod: RPN2106, GE Healthcare). Signals were quantified by densitometry analysis, adjusted relatively to ERK1/2 levels and graphed as OD fold change (mean ± SEM).

The specificity of immunoreaction has already been demonstrated (27, 28, 49, 51) and here routinely checked by omitting primary antibody (data not shown).

Statistical Analysis

Student's *t*-test or ANOVA followed by Duncan's test for multi-group comparison were performed, where appropriate, to evaluate the significance of differences. Data were expressed as the mean ± SEM.

RESULTS

Analysis of ECS Components During the First Wave of Spermatogenesis

The presence of ECS components has been investigated in rat testis by RT-PCR analyses. In particular, the expression profile for *Faah*, *Nape-pld*, *Magl*, *Dagl*, and *Cb2* mRNA has been analyzed from 7 to 60 dpp. The expression of *Cb1* in rat testis during the first spermatogenic wave has already been investigated by our group (49) and here just analyzed during perinatal period.

Results show that *Faah*, *Nape-pld*, *Magl*, *Dagl*, and *Actin* were constantly present in rat testis from 7 to 60 dpp. The **Figure 1A** shows one band of the predicted size for each transcript (see specific amplicons in **Table 1**). The **Figure 1B** shows representative agarose gel image of RT+ (testes from 90 dpp rats) and RT- (testes from 7 to 60 dpp rats) cDNA analyzed by PCR using actin primers.

Densitometry analysis of signals, normalized relatively to Actin, and graphed relatively to temporal profile of germ cells appearance or activities (**Figure 1C**), revealed specific fluctuations of gene expression (**Figure 1D**). At 7 dpp, *Faah* and *Nape-pld* were poorly expressed. Thereafter, *Faah* mRNA progressively and significantly increased up to 60 dpp ($p < 0.01$). *Nape-pld* mRNA was low with no significant increase from 7 to 21 dpp. Later, a significant increase was observed at 27 dpp ($p < 0.01$) with a progressive higher expression from 31 dpp forward. Interestingly, *Faah* mRNA was constantly higher when compared with *Nape-pld* suggesting that *Faah* expression was mainly activated during the spermatogenic wave to downregulated intra-testicular AEA levels, except to 7 and 41 dpp when matching *Nape-pld*/*Faah* mRNA values were observed suggesting intra-testicular increase of AEA. *Dagl* mRNA levels were high at 7–21 dpp and drastically reduced from 27 to 60 dpp ($p < 0.01$). *Vice versa*, *Magl* mRNA levels were low at 7–21 dpp and a progressive higher expression was observed from 27 dpp forward ($p < 0.01$), suggesting few intra-testicular 2-AG.

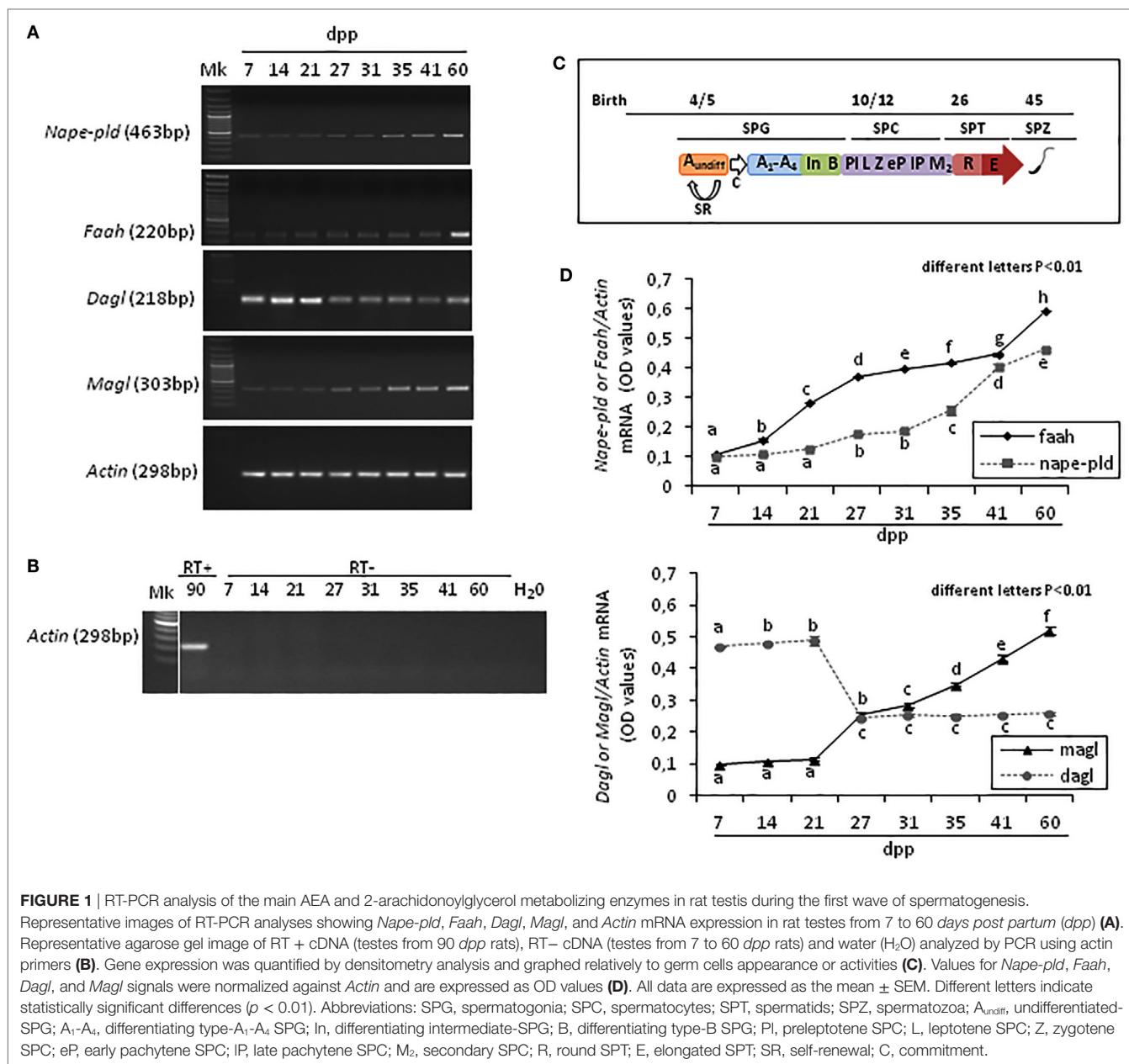
The presence of CB1 in fetal testis was studied by ICC at 14.5 and 19.5 dpc during proliferation and mitotic G1 arrest of germ cells, while the fluctuations of *Cb1* and *Cb2* mRNA were analyzed, using RT-PCR, during early *post-natal* period (from 1 to 14 dpp) and during all the spermatogenic wave (from 7 to 60 dpp), respectively.

In fetal testis, CB1 was absent at 14.5 dpc and present at 19.5 dpc. The protein was specifically related to gonocytes (**Figure 2A**). Specificity of immunoreactions has already been demonstrated and here checked again by omitting the primary antibody.

Transcripts for *Cb1*, *Cb2*, and *Actin* mRNA were present in testis. A single band of the predicted size for each transcript (see specific amplicons in **Table 1**) was obtained (upper panels **Figures 2B,C**). Densitometry analysis of signals, normalized relatively to *Actin*, revealed fluctuations of gene expression specifically related to each receptor (lower panels **Figures 2B,C**). *Cb1* mRNA was more highly expressed at 7 dpp (a vs b, $p < 0.01$) as compared to 1 and 14 dpp (**Figure 2B**). *Cb2* mRNA was feebly present at 7 dpp. Except to 41 dpp, its expression significantly and steadily increased from 7 to 60 dpp (different letters $p < 0.01$), with higher increases from 27 dpp onward (**Figure 2C**). The **Figure 2D** shows representative agarose gel image of RT+ (testes from 90 dpp rats) and RT- (testes from 1 to 60 dpp rats) cDNA analyzed by PCR using *Actin* primers.

Germ Cell Progression During the First Wave of Spermatogenesis

Specific molecular markers related to proliferation (66), meiosis (67), and differentiation (68) of germ cells were evaluated by RT-PCR analysis and conveniently correlated to ECS component expression during specific time frame of the first spermatogenic wave. In particular, *Cxcl12* was used as marker of SPG stem cell pool maintenance activity (2–14 dpp); *Mlh3* and a mouse testis-specific *Hsp70t*, were used as markers of appearance and presence of SPC (7–27 dpp) and SPT (21–60 dpp), respectively. *Actin* was analyzed as housekeeping gene. **Figure 3** shows (i) representative images of RT-PCR



analyses, (ii) graphs relative to densitometry analyses of signals (Figures 3A–C, upper panels), and (iii) appropriate correlation curves (Figures 3A–C, lower panels).

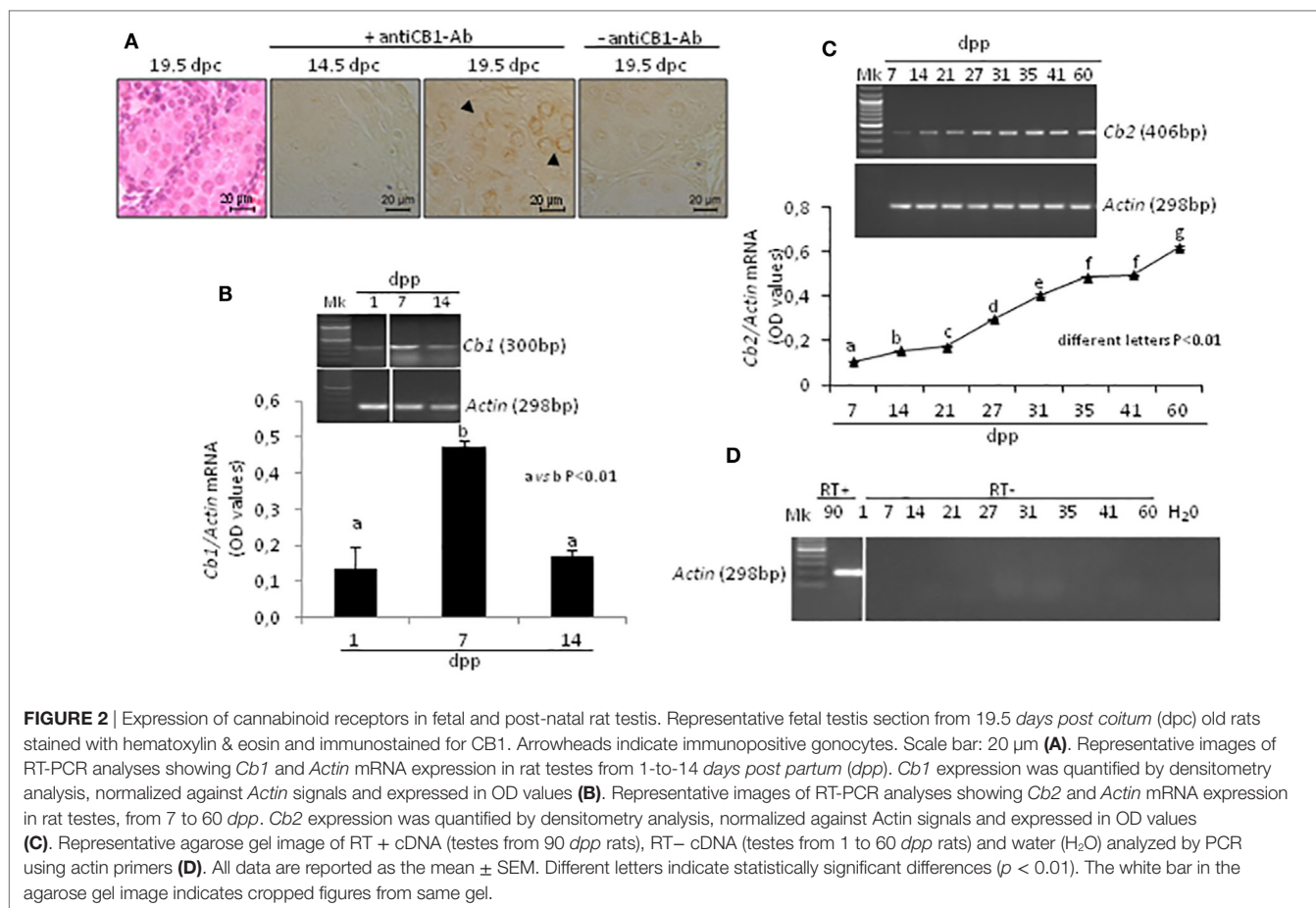
RT-PCR analysis confirmed the presence of *Cxcl12*, *Mlh3*, *Hsp70t*, and *Actin* mRNA as expected during the time frames specifically examined (i.e., mitotic, meiotic, differentiation phases). A single band of the predicted size for each transcript (see specific amplicons in Table 1) was obtained (upper panels Figures 3A–C). Densitometry analysis of signals, normalized relatively to *Actin*, revealed fluctuations of expression specifically related to each gene.

Cxcl12 mRNA was significantly higher at 7 dpp ($p < 0.01$) when compared with 1 and 14 dpp (Figure 3A, upper panels). The expression profiles of *Cxcl-12* and *Cb1* from 1 to 14 dpp

were positively and significantly correlated ($r = 0.67$, $p < 0.05$; Figure 3A lower panel).

At 7 dpp, *Mlh3* mRNA was absent. This first appeared at 14 dpp and increased steadily over the time (Figure 3B, upper panels). The expression profiles of *Mlh3* and *Cb2*, from 7 to 27 dpp, were positively and significantly correlated ($r = 0.94$, $p < 0.01$; Figure 3B, lower panel).

Hsp70t mRNA was absent at 21 dpp. It first appeared at 31 dpp and its expression levels increased progressively over time (Figure 3C, upper panels). The correlation analyses show that the expression profiles of *Hsp70t*, from 21 to 60 dpp, correlated positively and significantly with those of *Nape*, *Faah*, and *Magl* ($0.9 < r < 1$, $p < 0.01$) and negatively with the *Dagl/Magl* mRNA ratio ($r = -0.87$) (Figure 3C, lower panels).



Correlation Analyses Among ECS Components

Data on gene expression for *Nape-pld*, *Faah*, *Dagl*, *Magl*, and *Cb2*, from 21 to 60 dpp, have been used for correlation studies. Results show that the expression profiles of *Nape-pld*, *Magl*, and *Cb2* mRNA were positively and significantly correlated each other's ($0.88 < r < 0.96$; $p < 0.01$; **Figures 4A–C**). No significant correlation was found when the analysis was carried out using *Faah* or *Dagl* mRNA profiles (data not show).

Localization of ECS Components in Germ Cells

The expression of ECS components in germ cells has been analyzed in rat testis by ICC, using testes from 90 dpp rat. In particular, have been analyzed NAPE-PLD, FAAH, and MAGL proteins. ICC analysis show NAPE-PLD, FAAH, and MAGL proteins in Leydig cells (**Figure 5**). In tubular compartment, NAPE-PLD was feebly present in Sertoli cells and highly expressed in SPT and SPZ (**Figure 5A**). FAAH was present in germ cells, from preleptotene and pachytene SPC (_{PL}SPC and _PSPC) to round (r) and elongated (e) SPT (**Figure 5B**) while MAGL (**Figure 5C**) was feebly present in Sertoli cells associated to round SPT (stage IX/X), and in early condensing SPT (inset). Higher immunolocalization was observed in elongating SPT (eSPT).

Functional Interaction Among ECS Components

Testes from mice null of CB1 gene in heterozygous conditions (CB1^{+/-}) were used as model tissue of low levels of CB1 to verify responsiveness of expression of CB1 and MAGL proteins to AEA/CB2 activity. Testes CB1^{+/-} were incubated with vehicle or AEA, in presence/absence of AM630, a selective inverse agonist for CB2, and processed to quantify CB1 and MAGL proteins by Western blot analysis. Results are reported in **Figure 6**. Densitometry analysis of signals show that AEA significantly ($p < 0.05$) increased CB1 protein levels (**Figure 6B**) in comparison to control group, while a negative effect was observed ($p < 0.01$) on MAGL protein levels (**Figure 6C**). Both AEA-induced effects were efficiently counteracted by AM630 with different levels of statistical significance ($p < 0.05$ and $p < 0.01$).

DISCUSSION

The presence of ECS components has been investigated in rat testis during the first wave of spermatogenesis, from 7 to 60 dpp, to analyze the fluctuations of enzymes and receptors with respect to mitotic, meiotic, and post-meiotic germ cells. The expression profiles of the main enzymes metabolizing AEA and 2-AG (i.e., *Faah*, *Nape-pld*, *Magl*, *Dagl*), as well as the expression of CB receptors (*Cb1*, *Cb2*) and specific markers of germ cell presence

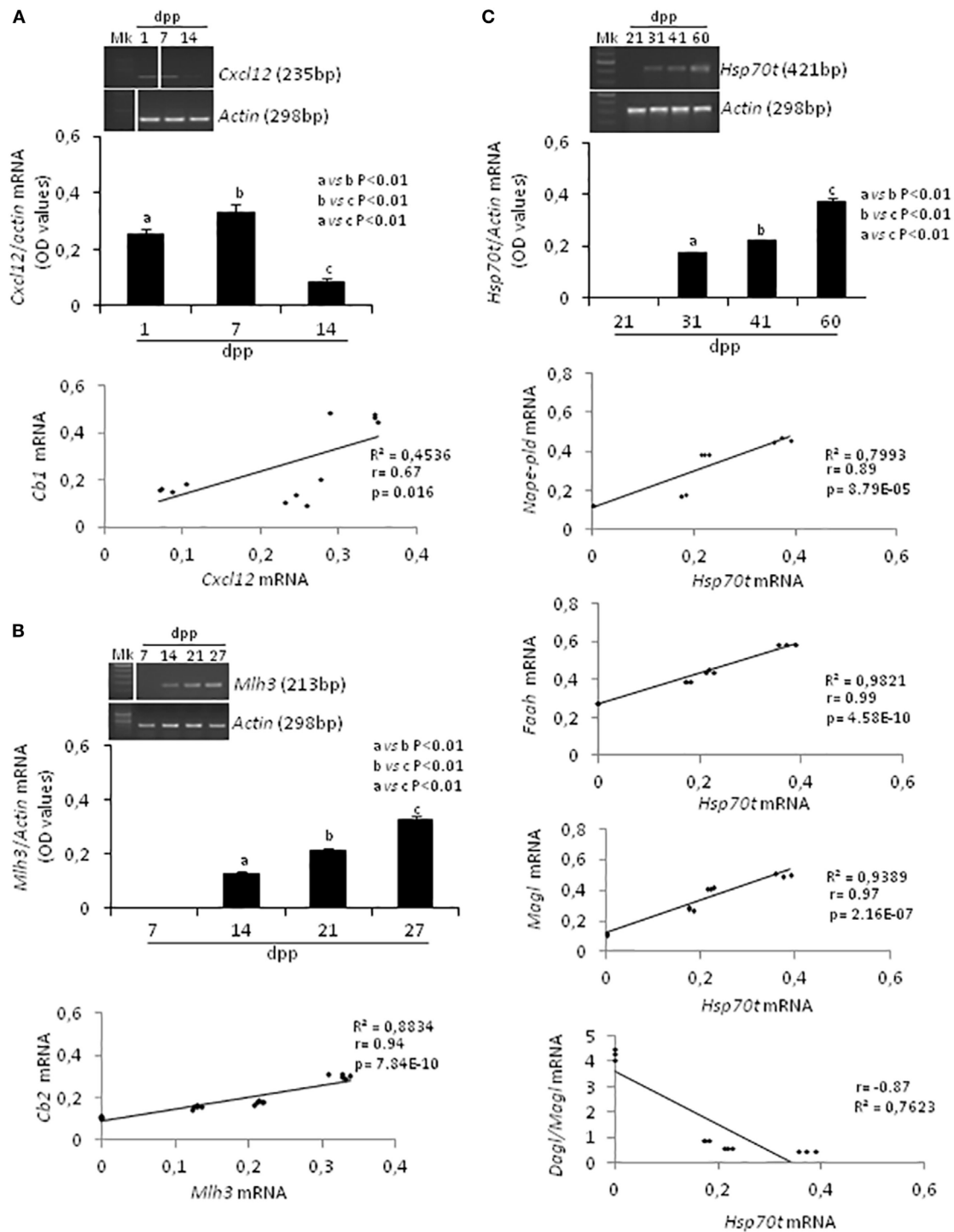
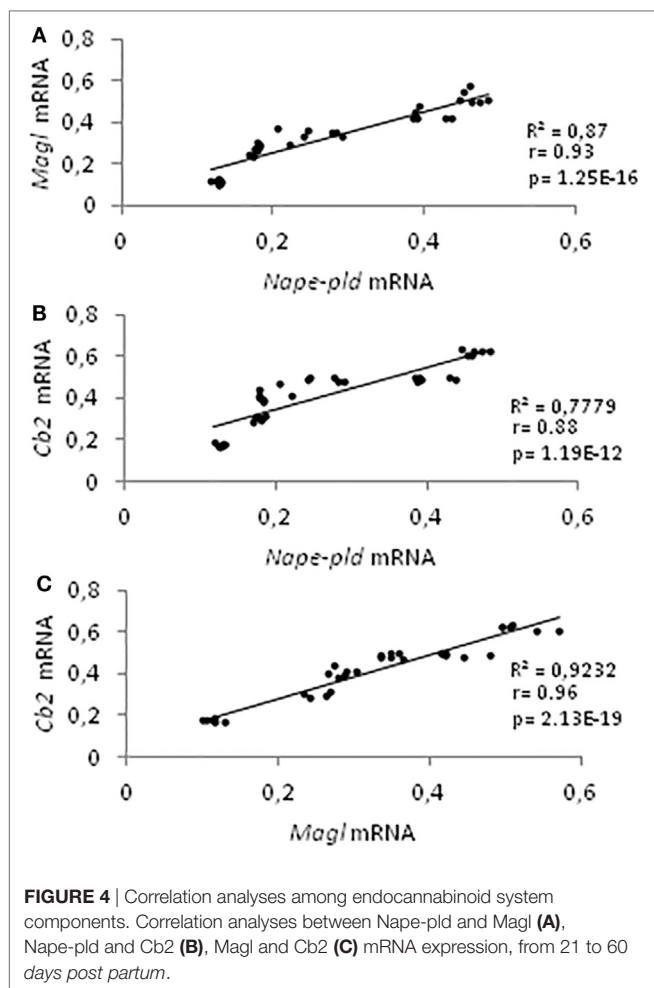


FIGURE 3 | RT-PCR analyses of specific markers related to the activity and/or presence of germ cells at specific times during the first spermatogenic wave and relative correlation analyses. Representative images of RT-PCR analyses showing *Cxcl12* and *Actin* mRNA expression in rat testis from 1 to 14 days post partum (dpp). *Cxcl12* expression was quantified by densitometry analysis and normalized against *Actin* signals. Values, expressed as OD have been used for correlation analysis between *Cxcl12* and *Cb1* mRNA expression (A). Representative images of RT-PCR analyses showing *Mlh3* and *Actin* mRNA expression in rat testis from 7 to 27 dpp. *Mlh3* expression was quantified by densitometry analysis and normalized against *Actin* signals. Values, expressed in OD, have been used for correlation analysis between *Mlh3* and *Cb2* mRNA expression (B). Representative images of RT-PCR analyses showing *Hsp70t* and *Actin* mRNA expression in rat testis from 21 to 60 dpp. *Hsp70t* expression was quantified by densitometry analysis and normalized against *Actin* signals. Values, expressed as OD, have been used for correlation analysis between *Hsp70t* and *Nape-pld* or *Faah* or *Magl* or *Dagl/Magl* mRNA expression (C). Different letters indicate statistically significant differences ($p < 0.01$). The white bars in the agarose gel images indicate cropped figures from same gel.



or activity have been analyzed by RT-PCR and appropriately correlated.

Results showed detailed fluctuations of gene expression. *Faah* and *Nape-pld* were poorly expressed at 7 *dpp*. Thereafter, *Faah* progressively and significantly increased up to 60 *dpp* while *Nape-pld* increased later, starting from 27 *dpp*. These data suggested that *Faah* expression was related to germ cell progression from SPG-to-SPT, while *Nape-pld* expression was more specifically related to SPT appearance. The high levels of *Faah* in SPC and SPT (*mRNA* and/or protein), when compared with SPG, have already been demonstrated in both frog and mouse (46, 50) and here confirmed by ICC analysis. Interestingly, *Faah* was consistently higher as compared with *Nape-pld*, except at 7 and 41 *dpp*, when similar *Nape-pld/Faah mRNA* levels were observed. This suggested that, during spermatogenesis progression, *Faah* was constantly expressed to control intra-testicular AEA levels, and that peaks of AEA specifically occurred in the testis during early and later phases of spermatogenesis. However, the expression profile of *Dagl* and *Magl* clearly showed that early phases of spermatogenesis required high intra-testicular 2-AG levels. *Vice versa*, lower amounts of 2-AG were necessary later. Accordingly, data from isolated mouse germ cells demonstrate that SPG produce more 2-AG due to the higher *Dagl* and lower *Magl* expression

(both *mRNA* and protein) when compared with meiotic and post-meiotic cells (50). In agreement, ICC analysis show that testis from rat at 90 *dpp* expressed MAGL in Leydig cells and appeared in tubular compartment later during spermatogenesis in Sertoli cells and SPT.

The expression profile of CB1 in rat testis, already investigated by our group during the first wave of spermatogenesis (49), was here analyzed in fetal and post-natal testis, with respect to gonocyte activity during their mitotic arrest (i.e., in G1 phase) and proliferative resumption. More specifically, we immunolocalized CB1 protein in fetal testis during proliferation (14.5 *dpc*) and mitotic arrest in G1 phase (19.5 *dpc*) of gonocytes, then we studied testicular fluctuations of *Cb1 mRNA* in *post-natal* testis, during the cell cycle arrest (1 *dpp*), mitotic resumption (7 *dpp*), and meiotic entry (14 *dpp*). The expression of *Cxcl12* (66) and *Mlh3* (67) was used to specifically define the activity of the SPG stem cell pool maintenance and the appearance of SPC, respectively. In addition, we studied the expression profile of *Cb2*, from 7 to 60 *dpp*, using *Hsp70t* (68) to specifically define SPT appearance from 21 *dpp* forward.

Data reported here show that CB1 was present in the testis at 19.5 *dpc*. The protein was exclusively localized in gonocytes. The lack of signals at 14.5 *dpc*, suggested that CB1 protein was functionally related to mitotic G1 arrest of germ cells (5) confirming the cytostatic activity of CB1 observed in Leydig cells (39). In agreement with data from mouse and rat (45, 49), the gene expression analysis carried out on post-natal testis revealed that *Cb1 mRNA* levels were low at 1 and 14 *dpp* and high at 7 *dpp*. Indeed, *Cb1* profile well correlated with *Cxcl12* profile and both matched specifically with post-natal fluctuations of AEA metabolizing enzymes suggesting that CB1 and a weak intra-testicular AEA rise were related to germ cell mitotic resumption. More specifically, the significant correlation of *Cb1* with *Cxcl12* suggested a potential involvement of CB1 in SPG stem cell pool maintenance activity (i.e., self-renewal activity and/or the relative commitment). However, *Cb1 mRNA* decreased at 14 *dpp* when type-A SPG were present in the testis and proliferating to become SPC. Interestingly, the impressive *Cb1* decrease was associated with the appearance of *Mlh3* which expression increased in correlation with *Cb2* and in presence of high *Dagl* and low *Magl mRNA* levels. This suggests that SPG proliferation and meiotic entry required the presence of CB2 and high levels of 2-AG. In agreement, Grimaldi and coworkers demonstrated that CB2 is highly expressed in mouse SPG, and its activation, likely *via* 2-AG, promotes meiotic entry (50). However, during later stages of spermatogenesis, at 27 *dpp*, the expression of ECS components changed drastically, in concomitance with the appearance of SPT. Indeed, the expression profile of *Hsp70t* demonstrated that SPT appeared between 21 and 31 *dpp* enriching progressively the germinal compartment. Simultaneously, a significant and gradual increase of *Nape-pld* and *Magl* was observed suggesting that, when in the testis *post-meiotic* germ cells are present (49), these cells might be or support the AEA source and play a key role in 2-AG degradation.

Data obtained in mouse show that SPT produce appreciable amount of AEA and that 2-AG is more efficiently synthesized in SPG when compared with SPC and SPT (50). Consistently, SPT result also to be the main producers of *Magl*, among germ cells (50). To verify these data in our animal model, we carried out

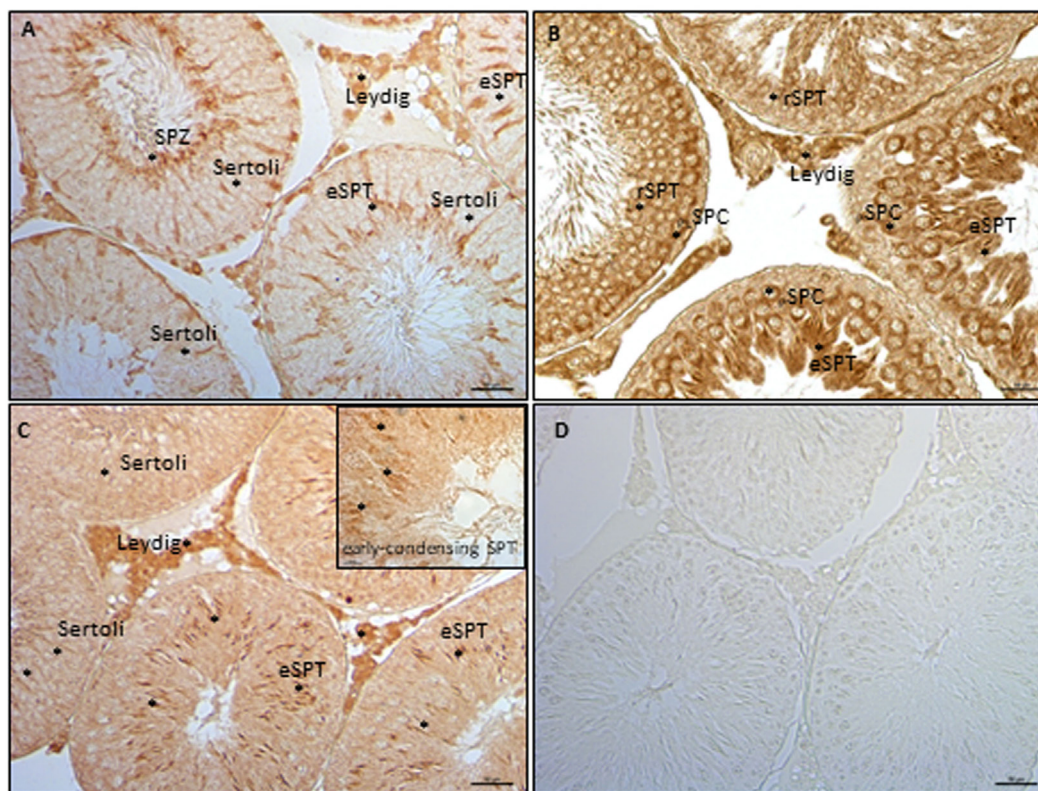


FIGURE 5 | Immunocytochemistry analyses of endocannabinoid system components in testis from rat at 90 days post partum. Immunolocalization of NAPE-PLD (A), fatty acid amide hydrolase (B), and monoacylglycerol-lipase (C) proteins in interstitial and tubular compartments. Asterisks indicate immunopositive cells. Specificity of reaction was checked by omitting the primary antibody (D). Scale bar: 50 μ m; inset scale bar: 10 μ m.

correlation analyses within the appropriate time frame, 21–60 *dpp*. Results showed that *Nape-pld*, *Faah*, and *Magl* fluctuations correlated positively with *Hsp70t* expression. In agreement, ICC analysis confirm higher expression of NAPE-PLD and FAAH proteins from round to elongated SPT, while MAGL feebly appeared in early condensing SPT and Sertoli cells and higher expressed in elongating SPT. A negative relation was observed when *Dagl/Magl* mRNA ratio, here used as indirect index of intra-testicular 2-AG levels, was correlated to expression of *Hsp70t*. The expression profiles of *Nape-pld*, *Magl*, and *Cb2* were positively correlated each other. We concluded that the appearance of SPT was directly or indirectly responsible of AEA synthesis and 2-AG hydrolysis.

Studies carried out on murine isolated germ cells and immature mouse demonstrate that CB2 signaling, likely responsive to 2-AG, controls meiotic entry (SPG/preleptotene-SPC differentiation) of SPG (50, 59). Interestingly, spermatogenic progression of more immature germ cells is responsive to feedback signals from more mature germ cells (13). Indeed, an intriguing testicular network of cell-to-cell communication controls progression of more mature and immature germ cells, properly clustered in specific stages. Intriguingly, in immature rat testis, CB1 appears in Sertoli cells in combination with the appearance of elongated SPT (22, 49). In mature rat testis, a weak and stage-specific expression of CB1 has been observed in Sertoli cells at stages VIII–IX/X (49) corresponding to Sertoli/SPC/elongated SPT-clustered cells. In frog

and rat, the presence of SPT is positively associated with the increase of CB1 (46, 49). In frog testis, CB1 expression is responsive to AEA (69). Therefore, we hypothesized that SPT control synthesis of AEA and that such a ligand, through activation of both CB receptors, affects 2-AG levels promoting meiotic entry of SPC. With this model in mind, we checked at molecular level, if AEA, *via* CB2, downregulated MAGL by inducing CB1 increase. Testis from mice null of CB1 in heterozygous condition (CB1^{+/-}) was used as model tissue of down-expression of CB1 (then potentially responsive to increase after stimulation) and stimulated with AEA \pm AM630. The aim was to verify the responsiveness of CB1 and MAGL protein expression to AEA/CB2 signaling. Results demonstrate that AEA-CB2 activity affected negatively MAGL levels *via* upregulation of CB1. This functional interaction of ECS components supports data above reported (i.e., low levels of *Magl* are present in the testis during mitotic/meiotic cell progression; high levels of *Nape-pld* are present in the testis when post-meiotic cells appear) and suggest their functional interaction (i.e., functional clustering) in testis during germ cell progression demonstrating a CB1/CB2-mediated relationship between AEA and 2-AG. Intriguingly, this might be the molecular network through which the appearance of elongated SPT control meiotic entry of SPC (13). Of course, further analyses should be specifically addressed to verify this model of cell-to-cell communication.

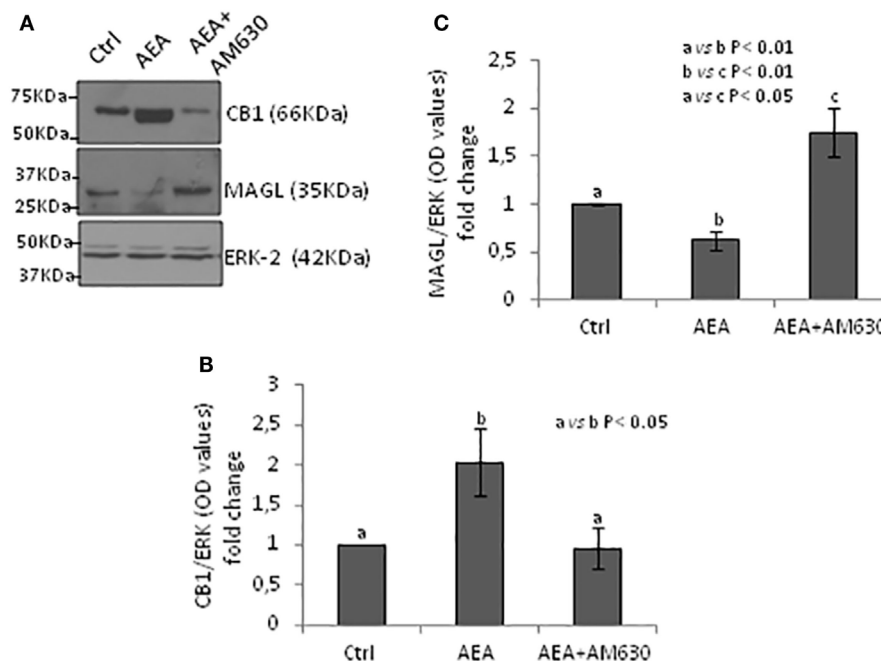


FIGURE 6 | Responsiveness of monoacylglycerol-lipase (MAGL) to CB1/CB2 receptors. Western blot analysis of CB1 and MAGL in CB1^{-/-} testes exposed to vehicle or AEA ± AM630 **(A)**. CB1 amount was quantified by densitometry analysis, normalized against ERK1/2 signals, and expressed in OD values as fold change **(B)**. MAGL amount was quantified by densitometry analysis, normalized against ERK1/2 signals, and expressed in OD values as fold change **(C)**. All data are reported as mean ± SEM.

Altogether, our data perfectly matches those obtained in isolated mouse germ cells (50) thus excluding species-specific differences (mouse vs rat) and reinforcing the rationale about our methodological choice (see Materials and Methods). Further analyses are necessary to specifically characterize the cells expressing CB receptors and enzymes metabolizing AEA and 2-AG to better define cellular network involved in local control of spermatogenesis. However, the above described observations are relevant since these show that *mRNA* level variations of ECS components are extremely robust, highly conserved, and functionally clustered during spermatogenesis. Accordingly, our data should be considered as identifying good molecular markers to follow a correct spermatogenesis progression. In this context, present data may open the possibility to develop algorithms for describing and monitoring testicular function. In the literature, spermatogenesis computational analysis, based on whole transcriptome, has already been described (70, 71). However, algorithms based on the expression levels of functionally clustered genes (as ECS components) might be a better and simpler way to monitor this complex event.

In conclusion, data here reported show that ECS components are functionally clustered and are differentially related to germ cell progression. In particular, CB2 and 2-AG appear to be related to mitotic/meiotic stages, while CB1 and AEA appear to be related to SPG stem cells activity and SPT appearance, respectively. We show that CB2 activity, stimulated *in vitro* by AEA, affects MAGL levels *via* upregulation of CB1, providing the first functional data supporting a CB1/CB2-mediated relationship between AEA and 2-AG. Furthermore, we show that fetal testis expresses CB1 providing, for the first time, evidence that the protein is present

in gonocytes blocked in mitosis. Finally, present data may shed light in the study of complex systems computational modeling.

ETHICS STATEMENT

Experiment were approved by the Italian Ministry of Education (MIUR) and the Italian Ministry of Health. All methods and all animal procedures were performed in accordance with the relevant guidelines and regulations by National Research Council's (NRC) for Care and Use of Laboratory Animals (NIH Guide).

AUTHOR CONTRIBUTIONS

TC, MM, GR, FM, and GC: conception and design of the work. TC and GC: manuscript drafting; AS: figures preparation. KM and GC: critical revision. SF and RP: final version approval.

ACKNOWLEDGMENTS

We thank Diego Dinucci (Animal Facility, Università della Campania) for animal care.

FUNDING

This work was supported by Italian Ministry of University and Research (Grant PRIN to GC 2010-2011), Regione Campania (Grant Legge 5/2007 to RP; Grant Legge 5/2008 to GC), Università della Campania (Grant 2017 Dip. Medicina Sperimentale to GC), and NIH (Grant DA021696 to KM).

REFERENCES

- Cobellis G, Noviello C, Nino F, Romano M, Mariscoli F, Martino A, et al. Spermatogenesis and cryptorchidism. *Front Endocrinol* (2014) 5:63. doi:10.3389/fendo.2014.00063
- Ricci G, Catizone A, Galdieri M. Pleiotropic activity of hepatocyte growth factor during embryonic mouse testis development. *Mech Dev* (2002) 118:19–28. doi:10.1016/S0925-4773(02)00247-2
- Ricci G, Catizone A, Galdieri M. Embryonic mouse testis development: role of platelet derived growth factor (PDGF-BB). *J Cell Physiol* (2004) 200:458–67. doi:10.1002/jcp.20035
- Spiller CM, Feng CW, Jackson A, Gillis AJ, Rolland AD, Looijenga LH, et al. Endogenous nodal signaling regulates germ cell potency during mammalian testis development. *Development* (2012) 139:4123–32. doi:10.1242/dev.083006
- Moreno SG, Dutrillaux B, Coffigny H. Study of the gonocyte cell cycle in irradiated TP53 knockout mouse fetuses and newborns. *Int J Radiat Biol* (2002) 78:703–9. doi:10.1080/09553000210134818
- Hess RA. Spermatogenesis: an overview. In: Knobil E, Neill JD, editors. *Encyclopedia of Reproduction*. San Diego; London; Boston; New York; Sydney; Tokyo; Toronto: Academic Press (1999). p. 539–45.
- Cacciola G, Chioccarelli T, Fasano S, Pierantoni R, Cobellis G. Estrogens and spermiogenesis: new insights from type 1 cannabinoid receptor knockout mice. *Int J Endocrinol* (2013) 2013:501350. doi:10.1155/2013/501350
- Sharpe RM. Paracrine control of the testis. *Clin Endocrinol Metab* (1986) 15:185–207. doi:10.1016/S0300-595X(86)80049-4
- Cobellis G, Pierantoni R, Minucci S, Pernas-Alonso R, Meccariello R, Fasano S. c-fos activity in *Rana esculenta* testis: seasonal and estradiol-induced changes. *Endocrinology* (1999) 140:3238–44. doi:10.1210/endo.140.7.6790
- O'Donnell L, Robertson KM, Jones ME, Simpson ER. Estrogen and spermatogenesis. *Endocr Rev* (2001) 22:289–318. doi:10.1210/er.22.3.289
- Cobellis G, Meccariello R, Fienga G, Pierantoni R, Fasano S. Cytoplasmic and nuclear Fos protein forms regulate resumption of spermatogenesis in the frog, *Rana esculenta*. *Endocrinology* (2002) 143:163–70. doi:10.1210/endo.143.1.8567
- Pierantoni R, Cobellis G, Meccariello R, Palmiero C, Fienga G, Minucci S, et al. The amphibian testis as model to study germ cell progression during spermatogenesis. *Comp Biochem Physiol B Biochem Mol Biol* (2002) 132:131–9. doi:10.1016/S1096-4959(01)00543-7
- Pierantoni R, Cobellis G, Meccariello R, Fasano S. Evolutionary aspects of cellular communication in the vertebrate hypothalamo-hypophysio-gonadal axis. *Int Rev Cytol* (2002) 218:69–141. doi:10.1016/S0074-7696(02)18012-0
- Cobellis G, Meccariello R, Minucci S, Palmiero C, Pierantoni R, Fasano S. Cytoplasmic versus nuclear localization of Fos-related proteins in the frog, *Rana esculenta*, testis: in vivo and direct in vitro effect of a gonadotropin-releasing hormone agonist. *Biol Reprod* (2003) 68:954–60. doi:10.1095/biolreprod.102.008938
- Cobellis G, Lombardi M, Scarpa D, Izzo G, Fienga G, Meccariello R, et al. Fra1 activity in the frog, *Rana esculenta*, testis: a new potential role in sperm transport. *Biol Reprod* (2005) 72:1101–8. doi:10.1095/biolreprod.104.036541
- Catizone A, Ricci G, Del Bravo J, Galdieri M. Hepatocyte growth factor modulates in vitro survival and proliferation of germ cells during postnatal testis development. *J Endocrinol* (2006) 191:559–70. doi:10.1677/joe.1.06528
- Carreau S, Bouraima-Lelong H, Delalande C. Estrogens: new players in spermatogenesis. *Repr Biol* (2011) 11:174–93. doi:10.1016/S1642-431X(12)60065-5
- Chianese R, Chioccarelli T, Cacciola G, Ciaramella V, Fasano S, Pierantoni R, et al. The contribution of lower vertebrate animal models in human reproduction research. *Gen Comp Endocrinol* (2011) 171:17–27. doi:10.1016/j.ygcen.2010.12.011
- Meccariello R, Fasano S, Pierantoni R, Cobellis G. Modulators of hypothalamic-pituitary-gonadal axis for the control of spermatogenesis and sperm quality in vertebrates. *Front Endocrinol* (2014) 5:135. doi:10.3389/fendo.2014.00135
- Meccariello R, Chianese R, Chioccarelli T, Ciaramella V, Fasano S, Pierantoni R, et al. Intra-testicular signals regulate germ cell progression and production of qualitatively mature spermatozoa in vertebrates. *Front Endocrinol* (2014) 5:69. doi:10.3389/fendo.2014.00069
- Wenger T, Ledent C, Csernus V, Gerendai I. The central cannabinoid receptor inactivation suppresses endocrine reproductive functions. *Biochem Biophys Res Commun* (2001) 284:363–8. doi:10.1006/bbrc.2001.4977
- Pierantoni R, Cobellis G, Meccariello R, Cacciola G, Chianese R, Chioccarelli T, et al. CB1 activity in male reproduction: mammalian and nonmammalian animal models. *Vitam Horm* (2009) 81:367–87. doi:10.1016/S0083-6729(09)81014-5
- Pierantoni R, Cobellis G, Meccariello R, Cacciola G, Chianese R, Chioccarelli T, et al. Testicular gonadotropin-releasing hormone activity, progression of spermatogenesis, and sperm transport in vertebrates. *Ann N Y Acad Sci* (2009) 1163:279–91. doi:10.1111/j.1749-6632.2008.03617.x
- Battista N, Meccariello R, Cobellis G, Fasano S, Di Tommaso M, Pirazzi V, et al. The role of endocannabinoids in gonadal function and fertility along the evolutionary axis. *Mol Cell Endocrinol* (2012) 355:1–14. doi:10.1016/j.mce.2012.01.014
- Grimaldi P, Di Giacomo D, Geremia R. The endocannabinoid system and spermatogenesis. *Front Endocrinol* (2013) 4:192. doi:10.3389/fendo.2013.00192
- Wang H, Dey SK, Maccarrone M, Jekyll and Hyde: two faces of cannabinoid signaling in male and female fertility. *Endocr Rev* (2006) 27:427–48. doi:10.1210/er.2006-0006
- Acone G, Trabucco E, Colacurci N, Cobellis L, Mackie K, Meccariello R, et al. Low type I cannabinoid receptor levels characterize placental villous in labouring delivery. *Placenta* (2009) 30:203–5. doi:10.1016/j.placenta.2008.11.018
- Trabucco E, Acone G, Marenga A, Pierantoni R, Cacciola G, Chioccarelli T, et al. Endocannabinoid system in first trimester placenta: low FAAH and high CB1 expression characterize spontaneous miscarriage. *Placenta* (2009) 30:516–22. doi:10.1016/j.placenta.2009.03.015
- Matsuda LA, Lolait SJ, Brownstein MJ, Young AC, Bonner TI. Structure of a cannabinoid receptor and functional expression of the cloned cDNA. *Nature* (1990) 346:561–4. doi:10.1038/346561a0
- Munro S, Thomas KL, Abu-Shaar M. Molecular characterization of a peripheral receptor for cannabinoids. *Nature* (1993) 365:61–5. doi:10.1038/365061a0
- Devane WA, Hanus L, Breuer A, Pertwee RG, Stevenson LA, Griffin G, et al. Isolation and structure of a brain constituent that binds to the cannabinoid receptor. *Science* (1992) 258:1946–9. doi:10.1126/science.1470919
- Sugiura T, Kondo S, Sukagawa A, Nakane S, Shinoda A, Itoh K, et al. 2-Arachidonoylglycerol: a possible endogenous cannabinoid receptor ligand in brain. *Biochem Biophys Res Commun* (1995) 215:89–97. doi:10.1006/bbrc.1995.2437
- Okamoto Y, Morishita J, Tsuboi K, Tonai T, Ueda N. Molecular characterization of a phospholipase D generating anandamide and its congeners. *J Biol Chem* (2004) 279:5298–305. doi:10.1074/jbc.M306642200
- Bisogno T, Howell F, Williams G, Minassi A, Cascio MG, Ligresti A, et al. Cloning of the first sn1-DAG lipases points to the spatial and temporal regulation of endocannabinoid signaling in the brain. *J Cell Biol* (2003) 163:463–8. doi:10.1083/jcb.200305129
- Dinh TP, Carpenter D, Leslie FM, Freund TF, Katona I, Sensi SL, et al. Brain monoglyceride lipase participating in endocannabinoid inactivation. *Proc Natl Acad Sci U S A* (2002) 99:13961. doi:10.1073/pnas.152334899
- McKinney MK, Cravatt BF. Structure and function of fatty acid amide hydrolase. *Annu Rev Biochem* (2005) 74:411–32. doi:10.1146/annurev.biochem.74.082803.133450
- Iannotti FA, Silvestri C, Mazzarella E, Martella A, Calvigioni D, Piscitelli F, et al. The endocannabinoid 2-AG controls skeletal muscle cell differentiation via CB1 receptor-dependent inhibition of Kv7 channels. *Proc Natl Acad Sci U S A* (2014) 111:E2472–81. doi:10.1073/pnas.1406728111
- Suglia A, Chianese R, Migliaccio M, Ambrosino C, Fasano S, Pierantoni R, et al. Bisphenol A induces hypothalamic down-regulation of the cannabinoid receptor 1 and anorexigenic effects in male mice. *Pharmacol Res* (2016) 113:376–83. doi:10.1016/j.phrs.2016.09.005
- Cacciola G, Chioccarelli T, Ricci G, Meccariello R, Fasano S, Pierantoni R, et al. The endocannabinoid system in vertebrate male reproduction: a comparative overview. *Mol Cell Endocrinol* (2008) 286:S24–30. doi:10.1016/j.mce.2008.01.004
- Bovolin P, Cottone E, Pomatto V, Fasano S, Pierantoni R, Cobellis G, et al. Endocannabinoids are involved in male vertebrate reproduction: regulatory mechanisms at central and gonadal level. *Front Endocrinol* (2014) 5:54. doi:10.3389/fendo.2014.00054
- Cacciola G, Chianese R, Chioccarelli T, Ciaramella V, Fasano S, Pierantoni R, et al. Cannabinoids and reproduction: a lasting and intriguing history. *Pharmaceuticals* (2010) 3:3275–323. doi:10.3390/ph3103275

42. Pertwee RG, Joe-Adigwe G, Hawksworth GM. Further evidence for the presence of cannabinoid CB1 receptors in mouse vas deferens. *Eur J Pharmacol* (1996) 296:169–72. doi:10.1016/0014-2999(95)00790-3
43. Maccarrone M, Ceconi S, Rossi G, Battista N, Pauselli R, Finazzi-Agro A. Anandamide activity and degradation are regulated by early postnatal aging and follicle-stimulating hormone in mouse Sertoli cells. *Endocrinology* (2003) 144:20–8. doi:10.1210/en.2002-220544
44. Maccarrone M, Barboni B, Paradisi A, Bernabò N, Gasperi V, Pistilli MG, et al. Characterization of the endocannabinoid system in boar spermatozoa and implications for sperm capacitation and acrosome reaction. *J Cell Sci* (2005) 118:4393–404. doi:10.1242/jcs.02536
45. Gye MC, Kang HH, Kang HJ. Expression of cannabinoid receptor 1 in mouse testes. *Arch Androl* (2005) 51:247–55. doi:10.1080/014850190898845
46. Cobellis G, Cacciola G, Scarpa D, Meccariello R, Chianese R, Franzoni MF, et al. Endocannabinoid system in frog and rodent testis: type-1 cannabinoid receptor and fatty acid amide hydrolase activity in male germ cells. *Biol Reprod* (2006) 75:82–9. doi:10.1095/biolreprod.106.051730
47. Ricci G, Cacciola G, Altucci L, Meccariello R, Pierantoni R, Fasano S, et al. Endocannabinoid control of sperm motility: the role of epididymus. *Gen Comp Endocrinol* (2007) 153:320–2. doi:10.1016/j.ygcen.2007.02.003
48. Rossi G, Gasperi V, Paro R, Barsacchi D, Ceconi S, Maccarrone M. Follicle-stimulating hormone activates fatty acid amide hydrolase by protein kinase A and aromatase-dependent pathways in mouse primary Sertoli cells. *Endocrinology* (2007) 148:431–9. doi:10.1210/en.2006-0969
49. Cacciola G, Chioccarelli T, Mackie K, Meccariello R, Ledent C, Fasano S, et al. Expression of type-1 cannabinoid receptor during rat postnatal testicular development: possible involvement in adult Leydig cell differentiation. *Biol Reprod* (2008) 79:758–65. doi:10.1095/biolreprod.108.070128
50. Grimaldi P, Orlando P, Di Siena S, Lolicato F, Petrosino S, Bisogno T, et al. The endocannabinoid system and pivotal role of the CB2 receptor in mouse spermatogenesis. *Proc Natl Acad Sci U S A* (2009) 106:11131–6. doi:10.1073/pnas.0812789106
51. Cobellis G, Ricci G, Cacciola G, Orlando P, Petrosino S, Cascio MG, et al. A gradient of 2-arachidonoylglycerol regulates mouse epididymal sperm cell start-up. *Biol Reprod* (2010) 82:451–8. doi:10.1095/biolreprod.109.079210
52. Rossato M, Ion Popa F, Ferigo M, Clar IG, Foresta C. Human sperm express cannabinoid receptor Cb1, the activation of which inhibits motility, acrosome reaction, and mitochondrial function. *J Clin Endocrinol Metab* (2005) 90:984–91. doi:10.1210/jc.2004-1287
53. Chianese R, Ciaramella V, Scarpa D, Fasano S, Pierantoni R, Meccariello R. Anandamide regulates the expression of GnRH1, GnRH2, and GnRH-Rs in frog testis. *Am J Physiol* (2012) 303:E475–87. doi:10.1152/ajpendo.00086.2012
54. Cacciola G, Chioccarelli T, Altucci L, Ledent C, Mason JI, Fasano S, et al. Low 17beta-estradiol levels in Cnr1 knock-out mice affect spermatid chromatin remodeling by interfering with chromatin reorganization. *Biol Reprod* (2013) 88:1–12. doi:10.1095/biolreprod.112.105726
55. Cacciola G, Chioccarelli T, Altucci L, Viggiano A, Fasano S, Pierantoni R, et al. Nuclear size as estrogen-responsive chromatin quality parameter of mouse spermatozoa. *Gen Comp Endocrinol* (2013) 193:201–9. doi:10.1016/j.ygcen.2013.07.018
56. Cobellis G, Meccariello R, Chianese R, Chioccarelli T, Fasano S, Pierantoni R. Effects of neuroendocrine CB1 activity on adult Leydig cells. *Front Endocrinol* (2016) 7:47. doi:10.3389/fendo.2016.00047
57. Chioccarelli T, Cacciola G, Altucci L, Lewis SE, Simon L, Ricci G, et al. Cannabinoid receptor 1 influences chromatin remodeling in mouse spermatids by affecting content of transition protein 2 mRNA and histone displacement. *Endocrinology* (2010) 151:5017–29. doi:10.1210/en.2010-0133
58. Francavilla F, Battista N, Barbonetti A, Vassallo MR, Rapino C, Antonangelo C, et al. Characterization of the endocannabinoid system in human spermatozoa and involvement of transient receptor potential vanilloid 1 receptor in their fertilizing ability. *Endocrinology* (2009) 150:4692–700. doi:10.1210/en.2009-0057
59. Di Giacomo D, De Domenico E, Sette C, Geremia R, Grimaldi P. Type 2 cannabinoid receptor contributes to the physiological regulation of spermatogenesis. *FASEB J* (2016) 30:1453–63. doi:10.1096/fj.15-279034
60. Ledent C, Valverde O, Cossu G, Petitet F, Aubert JF, Beslot F, et al. Unresponsiveness to cannabinoids and reduced addictive effects of opiates in CB1 receptor knockout mice. *Science* (1999) 283:401–4. doi:10.1126/science.283.5400.401
61. Santangeli S, Maradonna F, Gioacchini G, Cobellis G, Piccinetti CC, Dalla Valle L, et al. BPA-induced deregulation of epigenetic patterns: effects on female zebrafish reproduction. *Sci Rep* (2016) 6:21982. doi:10.1038/srep21982
62. Crispi S, Calogero RA, Santini M, Mellone P, Vincenzi B, Citro G, et al. Global gene expression profiling of human pleural mesotheliomas: identification of matrix metalloproteinase 14 (MMP-14) as potential tumour target. *PLoS One* (2009) 4:e7016. doi:10.1371/journal.pone.0007016
63. Hsieh C, Brown S, Derleth C, Mackie K. Internalization and recycling of the CB1 cannabinoid receptor. *J Neurochem* (1999) 73:493–501. doi:10.1046/j.1471-4159.1999.0730493.x
64. Ross RA, Brockie HC, Stevenson LA, Murphy VL, Templeton F, Makriyannis A, et al. Agonist-inverse agonist characterization at CB1 and CB2 cannabinoid receptors of L759633, L759656, and AM630. *Br J Pharmacol* (1999) 126:665–72. doi:10.1038/sj.bjp.0702351
65. Bolognini D, Cascio MG, Parolaro D, Pertwee RG. AM630 behaves as a protean ligand at the human cannabinoid CB2 receptor. *Br J Pharmacol* (2012) 165:2561–74. doi:10.1111/j.1476-5381.2011.01503.x
66. Yang QE, Kim D, Kaucher A, Oatley MJ, Oatley JM. CXCL12-CXCR4 signaling is required for the maintenance of mouse spermatogonial stem cells. *J Cell Sci* (2013) 126:1009–20. doi:10.1242/jcs.119826
67. Lipkin SM, Moens PB, Wang V, Lenzi M, Shanmugarajah D, Gilgeous A, et al. Meiotic arrest and aneuploidy in MLH3-deficient mice. *Nat Genet* (2002) 31:385–90. doi:10.1038/ng931
68. Ito Y, Ando A, Ando H, Ando J, Saijoh Y, Inoko H, et al. Genomic structure of the spermatid-specific hsp70 homolog gene located in the class III region of the major histocompatibility complex of mouse and man. *J Biochem* (1998) 124:347–53. doi:10.1093/oxfordjournals.jbchem.a022118
69. Ciaramella V, Meccariello R, Chioccarelli T, Sirleto M, Fasano S, Pierantoni R, et al. Anandamide acts via kisspeptin in the regulation of testicular activity of the frog, *Pelophylax esculentus*. *Mol Cell Endocrinol* (2016) 420:75–84. doi:10.1016/j.mce.2015.11.011
70. Cappallo-Obermann H, Feig C, Schulze W, Spiess AN. Fold-change correction values for testicular somatic transcripts in gene expression studies of human spermatogenesis. *Hum Reprod* (2013) 28:590–8. doi:10.1093/humrep/des433
71. Margolin G, Khil PP, Kim J, Bellani MA, Camerini-Otero RD. Integrated transcriptome analysis of mouse spermatogenesis. *BMC Genomics* (2014) 15:39. doi:10.1186/1471-2164-15-39

Conflict of Interest Statement: The authors declare that the research was conducted in the absence of any commercial or financial relationships that could be construed as a potential conflict of interest.

Copyright © 2018 Migliaccio, Ricci, Suglia, Manfredola, Mackie, Fasano, Pierantoni, Chioccarelli and Cobellis. This is an open-access article distributed under the terms of the Creative Commons Attribution License (CC BY). The use, distribution or reproduction in other forums is permitted, provided the original author(s) and the copyright owner are credited and that the original publication in this journal is cited, in accordance with accepted academic practice. No use, distribution or reproduction is permitted which does not comply with these terms.